AGU PUBLICATIONS

Geophysical Research Letters

RESEARCH LETTER
10.1002/2017GL073070

Key Points:
- Same activation volume of the mobility of rate-limiting process of [100](010) and [001](010) dislocations
- Pressure cannot cause olivine fabric transition from A type to B type
- The olivine AG-type fabric may be produced by low stress

Correspondence to:
L. Wang,
lin.wang@uni-bayreuth.de

Citation:
Wang, L., S. Blaha, T. Kawazoe, N. Miyajima, and T. Katsura (2017), Identical activation volumes of dislocation mobility in the [100](010) and [001](010) slip systems in natural olivine, *Geophys. Res. Lett.*, *44*, 2687–2692, doi:10.1002/2017GL073070.

Received 12 AUG 2016
Accepted 7 MAR 2017
Accepted article online 15 MAR 2017
Published online 22 MAR 2017

Identical activation volumes of dislocation mobility in the [100](010) and [001](010) slip systems in natural olivine

Lin Wang[1], Stephan Blaha[1], Takaaki Kawazoe[1], Nobuyoshi Miyajima[1], and Tomoo Katsura[1]

[1]Bayerisches Geoinstitut, Universität Bayreuth, Bayreuth, Germany

Abstract Dislocation recovery experiments were performed on predeformed olivine single crystals at pressures of 2, 7 and 12 GPa and a constant temperature of 1650 K to determine the pressure dependence of the annihilation rate constants for [100](010) edge dislocation (***a*** dislocation) and [001](010) screw dislocation (***c*** dislocation). The constants of both types of dislocations are comparable within 0.3 orders of magnitude. The activation volumes of ***a*** and ***c*** dislocations are small and identical within error: 2.7 ± 0.2 and 2.5 ± 0.9 cm^3/mol, respectively. These values are slightly larger and smaller than those of Si lattice and grain-boundary diffusions in olivine, respectively. The small and identical activation volumes for the ***a*** and ***c*** dislocations suggest that the pressure-induced fabric transition is unlikely in the asthenosphere. The decrease in seismic anisotropy with depth down in the asthenosphere may be caused by the fabric transition from A type or B type to AG type with decreasing stress with depth.

1. Introduction

A number of seismological studies showed anisotropy in seismic wave velocity in the Earth's upper mantle [*Dziewonski and Anderson*, 1981; *Montagner and Kennett*, 1996; *Gung et al*., 2003; *Nettles and Dziewonski*, 2008; *Visser et al*., 2008]. The upper mantle seismic anisotropy is interpreted by the lattice preferred orientations (LPO) and elastic anisotropy of olivine [e.g., *Karato*, 2012]. Some studies [e.g., *Gung et al*., 2003; *Visser et al*., 2008] depicted that the seismic anisotropy quickly decreases with increasing depth down to 300 km. The origin of this decrease is an issue of debate [e.g., *Karato*, 1992; *Mainprice et al*., 2005; *Raterron et al*., 2009]. Since elastic anisotropy of minerals is essentially independent from physical and chemical conditions, the decrease in seismic anisotropy should be resulted from weakening or change in LPO patterns (i.e., fabric transition).

Formation of LPO is a consequence of movement of dislocations of the dominant slip system(s) in dislocation creep. Therefore, if the decrease in seismic anisotropy with depth is caused by the change in LPO pattern, the dominant slip system should change with pressure. Several deformation experiments [*Couvy et al*., 2004; *Raterron et al*., 2007, 2009; *Jung et al*., 2009; *Raterron et al*., 2011; *Ohuchi et al*., 2011] showed that, although the transition pressure is under debate, the olivine fabric changes from A type to B type with increasing pressure. These results imply that the dominant slip system would change from [100](010) to [001](010), which are hereafter called ***a*** and ***c*** slips, respectively, with depth. These articles explained the decrease in seismic anisotropy by this fabric transition. However, further investigation is necessary to verify this hypothesis because the stress magnitude in their deformation experiments is by many orders of magnitude higher than that in asthenospheric conditions [*Hirth and Kohlstedt*, 2003], which may change the rate-limiting process of dislocation creep [*Wang et al*., 2016].

Our previous study [*Wang et al*., 2016] provided a different explanation. We reported identical dislocation mobility between ***a*** and ***c*** dislocations in the recovery process in olivine along elevating temperatures at an ambient pressure. The result indicates that there is no clear dominance between these two slip systems under low-stress conditions. Based on these observations, we proposed a new hypothesis that the decrease in seismic anisotropy may be caused by the fabric transition from A or B type to AG type with decreasing stress.

If the dislocation mobility of ***a*** and ***c*** slips has strong and different pressure dependence, *Wang et al*.'s [2016] hypothesis for the origin of the decrease in seismic anisotropy should be reconsidered. Therefore, the pressure dependence of dislocation mobility of the ***a***- and ***c***-slip systems must be investigated. In this

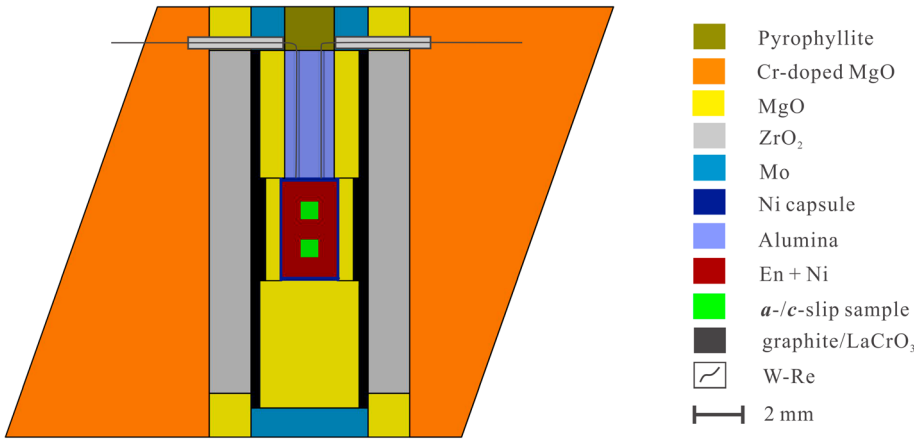

Figure 1. The sample assembly used in the multianvil high-pressure annealing experiments.

study, we conducted dislocation recovery experiments for ***a*** and ***c*** dislocations at various pressures and a constant temperature by a similar method to that of *Wang et al*. [2016] and determined the activation volumes of the annihilation rate constants for these two dislocations. As was the case in *Wang et al*. [2016], it is assumed that the average dislocation velocity is proportional to the dislocation mobility, which is proportional to the dislocation annihilation rate constant. Therefore, we can estimate the pressure dependences of the dislocation average velocity from those of dislocation annihilation rate constants. Our results show that the activation volumes are small and identical, and therefore, pressure cannot induce the fabric transition.

2. Experimental Procedure

The experimental procedure adopted in this study is similar to that of *Wang et al*. [2016] except two differences. One is that annealing was performed at high pressures of 2, 7, and 12 GPa and a constant temperature of 1650 K using a multianvil press, whose sample assembly is shown in Figure 1. Two olivine single crystals in which ***a*** and ***c*** dislocations were activated, respectively, in preceding simple shear deformation experiments were loaded together in a Ni capsule. The simple shear deformation experiment setup and procedure can be found in *Wang et al*. [2016]. The dominance of ***a*** and ***c*** dislocations in the deformed sample was confirmed by previous study [*Wang et al*., 2016]. The deformed samples were surrounded by a mixture of Ni and enstatite powders with a volume ratio of 1:1 to produce a quasi-hydrostatic condition and fix the oxygen fugacity at the Ni-NiO buffer and the SiO_2 activity of $a_{opx} = 1$. In order to test the effect of cold compression to the dislocation multiplication, we check the dislocation density increase of an undeformed sample which was cold compressed in the same experimental setup to 12 GPa. The H_2O contents in the samples were measured vertically to the (001) plane by unpolarized Fourier transform infrared spectroscopy before and after annealing based on the *Paterson*'s [1982] calibration. The other difference is that paired olivine crystals, each of which shared a common (001) plane, were used to precisely determine change in dislocation density by annealing. One piece from each pair was used to determine the initial dislocation density (as-crept piece), while the other was used to determine it after annealing (annealed piece). We counted dislocations in the corresponding areas of the paired as-crept and annealed pieces from the same group.

3. Results

Table 1 shows experimental results together with the annealing conditions. The dislocation density of the undeformed olivine cold compressed to 12 GPa is 0.03 μm^{-2}, which is much smaller than the dislocation density of ***a*** and ***c*** samples after annealing. Therefore, the effect of cold compression is negligible. Figure 2 shows backscattered electron images (BEI) of the oxidation-decorated dislocations before and after annealing. We measured water contents of three samples before and after annealing at 2 and 12 GPa, which are 13 ± 6 wt ppm. Because of small difference in water contents between low- and high-pressure annealed samples, the effects of water on dislocation annihilation are ignored in this study.

Table 1. Summary of Experimental Conditions and Results

Sample	*P* (GPa)	Annealing time (*t*, h)	Area	ρ_i^a (μm^{-2})	ρ_f^b (μm^{-2})	Log (*k*, $m^2 s^{-1}$)[c]
			[100](010) Edge Dislocation			
H3998-1	12	23.7	1	0.85 ± 0.25	0.48 ± 0.10	−17.2 ± 0.4
			2	2.47 ± 0.41	0.85 ± 0.19	−17.0 ± 0.2
H3998-2	7	10.7	1	1.22 ± 0.29	0.60 ± 0.14	−16.7 ± 0.2
			2	0.86 ± 0.30	0.54 ± 0.14	−16.8 ± 0.4
H3998-3	2	5.1	1	0.55 ± 0.10	0.33 ± 0.10	−16.2 ± 0.3
Z1253-1	2	6.0	1	2.28 ± 0.05	0.66 ± 0.15	−16.3 ± 0.1
			[001](010) Screw Dislocation			
Z1160-1	12	23.7	1	0.52 ± 0.17	0.24 ± 0.09	−16.6 ± 0.3
			2	2.01 ± 0.19	0.67 ± 0.14	−16.9 ± 0.1
Z1160-2	7	10.7	1	0.66 ± 0.07	0.47 ± 0.09	−16.8 ± 0.3
			2	0.79 ± 0.11	0.40 ± 0.10	−16.5 ± 0.2
Z1160-3	2	5.1	1	0.70 ± 0.17	0.46 ± 0.10	−16.4 ± 0.3
Z1247-1	2	6	1	0.16 ± 0.03	0.09 ± 0.04	−15.6 ± 0.5
Z1247-2	2	6	1	0.13 ± 0.01	0.10 ± 0.01	−16.0 ± 0.3

[a]Dislocation density before annealing.
[b]Dislocation density after annealing.
[c]$k = (1/\rho_f - 1/\rho_i)/t$.

Figure 3 plots the logarithm of the annihilation rate constants against pressure. The results from previous studies about dislocation recovery on olivine single crystals [*Kohlstedt et al.*, 1980; *Karato and Ogawa*, 1982; *Karato et al.*, 1993] are also plotted after temperature correction to 1650 K with an activation energy of 400 kJ/mol and activation volume of 2.7 cm^3/mol. The annihilation rate constants of ***a*** and ***c*** dislocations are comparable, but those for the ***c*** dislocation are by 0.3 orders of magnitude higher than those for the ***a*** dislocation. The activation volumes of dislocation annihilation rate constants in these two slip systems are both small and identical within the error: $V_a = 2.7 \pm 0.2$ and $V_c = 2.5 \pm 0.9$ cm^3/mol for ***a*** and ***c*** dislocations, respectively.

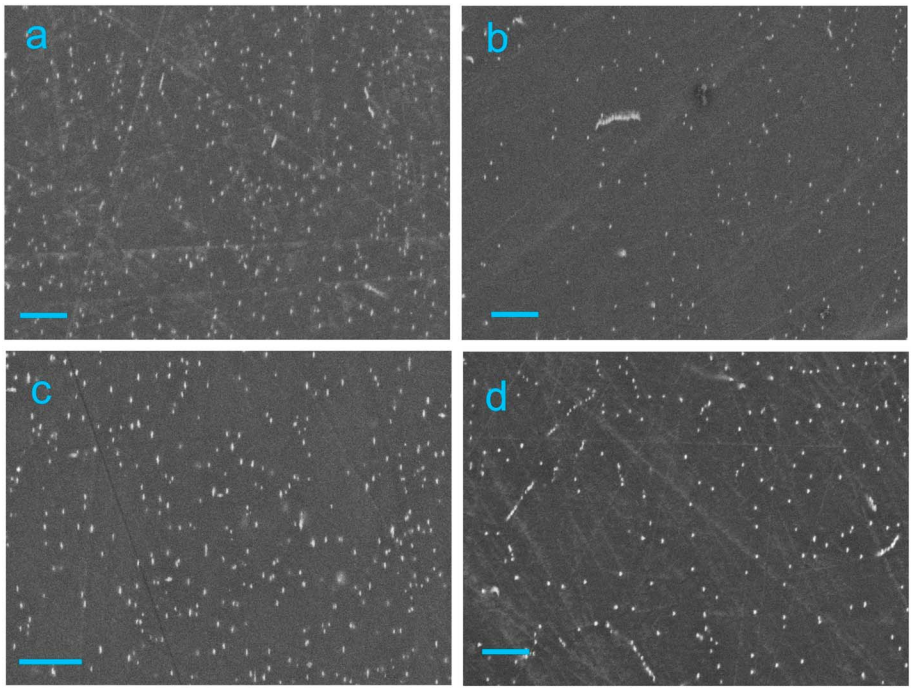

Figure 2. BEIs showing the dislocation density before and after annealing at 12 GPa for 24 h. The images were taken on the (001) plane. (a) ***a***-slip sample before annealing. (b) ***a***-slip sample after annealing. (c) ***c***-slip sample before annealing. (d) ***c***-slip sample after annealing. The scale bar shown represents 2 μm.

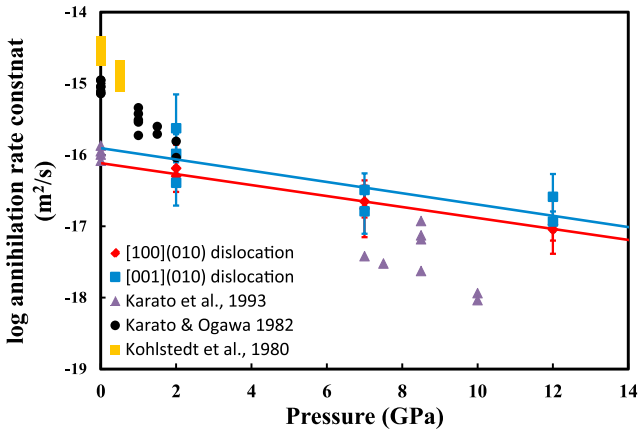

Figure 3. Logarithmic dislocation annihilation rate constants of ***a*** and ***c*** dislocations versus the pressure. No transition between ***a***- and ***c***-slip dislocation mobility occurs. Together plotted are the annihilation rate constants from previous studies corrected by activation energy of 400 kJ/mol and activation volume of 2.7 cm^3/mol.

4. Discussion

4.1. Diffusion-Controlled Dislocation Motion in Recovery Process

The ***a*** and ***c*** dislocations have comparable magnitudes of the annihilation rate constants and also the identical activation volumes. *Wang et al*. [2016] also demonstrated that they have identical activation energies (400 ± 20 and 400 ± 30 kJ/mol, respectively). These observations indicate that the rate-limiting process of dislocation motion in dislocation recovery process is isotropic and independent from the dislocation character at low stress. Moreover, the activation energy and volume of the Si lattice diffusion are 410 ± 30 kJ/mol and 1.7 ± 0.4 cm^3/mol, respectively, in forsterite [*Fei et al*., 2012], which are identical and comparable to those of the dislocation annihilation rate constants of olivine. Furthermore, *Jaoul et al*. [1981] demonstrated that the Si lattice diffusion is isotropic in forsterite. These facts reinforce that the rate-limiting process of dislocation recovery process is Si diffusion, as already discussed by *Wang et al*. [2016].

4.2. Comparison With Previous Studies

The activation volumes obtained in this study are considerably smaller than those by previous studies, namely 11 ± 1 cm^3/mol by *Kohlstedt et al*. [1980], 14 ± 2 cm^3/mol by *Karato and Ogawa* [1982], and 6 ± 1 cm^3/mol by *Karato et al*. [1993]. In *Kohlstedt et al*. [1980] and *Karato and Ogawa* [1982], the pressure range is only 0.5 and 2 GPa, respectively, which is too narrow to give accurate activation volume. In *Karato et al*. [1993], their activation volumes were obtained by comparing high-pressure data with ambient pressure ones. The differences in their experimental setups between high-pressure and ambient-pressure experiments could cause some discrepancy in obtained values, which might have biased the pressure dependence in these studies. On the other hand, the annihilation rate constants were obtained in the same experimental setup over the wide pressure interval of 10 GPa in this study, which allows robust estimation of the activation volumes. The rate constants of ***a*** dislocation from this study are slightly higher than the high-pressure data of *Karato et al*. [1993], which used the same technique as the present study to investigate the annihilation of ***a*** dislocation. One possible explanation for the discrepancy is that their annealing time was longer than ours. With increasing annealing time, all mobile dislocations with opposite sign nearly annihilate and the proportion of immobile dislocation increases. The phenomenon can lower apparent dislocation annihilation rate. This point can be proved by noticing that their results with short annealing time give high rate constants which are consistent with ours (their Table 1, 8.5 GPa data). The rate constants from *Kohlstedt et al*. [1980] and *Karato and Ogawa* [1982] are higher than those of ***c*** dislocation in this study. This may be due to different technique in counting dislocations. *Kohlstedt et al*. [1980] conducted transmission electron microscopy (TEM) observation in restricted sample areas, which made it difficult to obtain statistical averages when calculating dislocation annihilation rate constant. Optical microscopy [*Karato and Ogawa*, 1982] may underestimate dislocation density when it is high and was applied equally to obtain both initial and annealed dislocation density, which could have given higher annihilation rate constants.

4.3. Comparison With Other Techniques

Although we argued that the activation volumes of the dislocation annihilation rate constants in this study are comparable with that of Si self-diffusion given by *Fei et al*. [2012] (1.7 ± 0.4 cm^3/mol) in forsterite, they are slightly higher. On the other hand, the activation volume of the Si grain-boundary diffusion in forsterite is 4.0 ± 0.4 cm^3/mol [*Fei et al*., 2016], which is higher than those of the dislocation annihilation and Si lattice

diffusion. The lattice diffusion, dislocation climb, and grain-boundary diffusion are interactions between atoms and vacancy, dislocation, and grain boundary, respectively. Accordingly, it seems that the activation volume increases with increasing defect dimension. The higher-dimensional defect should have more loose structure, which may cause the larger activation volumes.

Deformation experiments on olivine single crystal by *Raterron et al*. [2009] yielded different activation volumes for ***a***- and ***c***-slip samples (12 ± 4 and 3 ± 4 cm^3/mol, respectively). This may be due to the large uncertainty of stress conditions in their experiments and fitting the results from their own high-pressure data and *Bai et al*.'s [1991] room-pressure data. Although both studies deformed olivine single crystals in the same orientations, their different experimental setups may have biased the result. Moreover, since both ***a*** and ***c*** dislocations elongate in the [001] direction and move in the same directions during glide and climb/cross slip, the activation volumes should be identical, as is shown by this study. Deformation experiments on olivine aggregate [*Karato and Rubie*, 1997; *Karato and Jung*, 2003; *Kawazoe et al*., 2009] showed that the activation volume for olivine creep is larger than 10 cm^3/mol. However, the stress conditions in these experiments are about 1 GPa, which is much higher than those in asthenospheric mantle. Therefore, the mechanism of olivine creep in such experiments may not be applicable to low-stress conditions [*Wang et al*., 2016]. *Couvy et al*. [2004] suggested that C or B type olivine fabric should be dominant at a pressure of 11 GPa and a temperature of 1400°C. However, we note that their olivine fabrics at high temperature were developed during stress relaxation from cold compression which produced dislocations only with the [001] Burgers vector at stresses about 1.5 GPa. Such experiments do not allow to prove dominance of the dislocations with the [001] Burgers vector at 1400°C and 11 GPa in the low-stress mantle conditions.

4.4. Geophysical Application

The identical activation volumes of the ***a*** and ***c*** dislocations motion lead to the same pressure dependence of olivine creep caused by ***a*** and ***c*** dislocations. Therefore, our results suggest that the pressure-induced LPO transition by these two types of dislocations is unlikely in asthenospheric mantle, on the assumption that dislocation creep and dislocation recovery are rate limited by the same physical mechanisms in the low-stress mantle conditions. Moreover, the small activation volumes suggest that the pressure effects on creep are small. For example, 10 GPa increase of pressure only causes decrease of creep rate by a factor of 5 at 1650 K by using activation energy of 400 kJ/mol [*Wang et al*., 2016].

The comparable rate constants, the identical activation energy and volumes [this study and *Wang et al*., 2016] of ***a***- and ***c***-dislocations recovery indicate that the rate-limiting process of these two dislocations have similar mobilities under low-stress conditions. Under such conditions, the free dislocation velocity should be equal to the velocity of dislocation motion in the rate-limiting process [*Boioli et al*., 2015; *Wang et al*., 2016] and AG-type fabric should be dominant [*Wang et al*., 2016]. Therefore, the decrease in seismic anisotropy with depth may be explained by the olivine LPO transition from A or B type to AG type by decrease in stress with depth [*Wang et al*., 2016].

Finally, we note that the effects of water and grain/phase boundary on dislocation mobility are necessary to be investigated in order to provide a better explanation for the LPO development in the Earth's mantle.

Acknowledgments
The data used are listed in Table 1 and the references. We acknowledge F. Heidelbach and P. O'Brien for providing the olivine single crystals and T. Boffa Ballaran for instructing the single crystal X-ray diffractometry. We thank technical assistance in BGI for the sample and assembly preparation. This research was supported by Deutsche Forschungsgemeinschaft grants to T.K. (KA3434/3-1, KA3434/7-1, KA3434/8-1, and KA3434/9-1) and by the annual budget of BGI.

References

Bai, Q., S. J. Mackwell, and D. L. Kohlstedt (1991), High-temperature creep of olivine single crystals 1. Mechanical results for buffered samples, *J. Geophys. Res.*, *96*(B2), 2441–2463.

Boioli, F., P. Carrez, P. Cordier, B. Devincre, and M. Marquille (2015), Modeling the creep properties of olivine by 2.5-dimensional dislocation dynamics simulations, *Phys. Rev. B*, *92*(1), doi:10.1103/PhysRevB.92.014115.

Couvy, H., D. J. Frost, F. Heidelbach, K. Nyilas, T. Ungar, S. Mackwell, and P. Cordier (2004), Shear deformation experiments of forsterite at 11 GPa–1400 C in the multianvil apparatus, *Eur. J. Mineral.*, *16*(6), 877–889.

Dziewonski, A. M., and D. L. Anderson (1981), Preliminary reference Earth model, *Phys. Earth Planet. Inter.*, *25*(4), 297–356.

Fei, H., C. Hegoda, D. Yamazaki, M. Wiedenbeck, H. Yurimoto, S. Shcheka, and T. Katsura (2012), High silicon self-diffusion coefficient in dry forsterite, *Earth Planet. Sci. Lett.*, *345–348*, 95–103.

Fei, H., S. Koizumi, N. Sakamoto, M. Hashiguchi, H. Yurimoto, K. Marquardt, N. Miyajima, D. Yamazaki, and T. Katsura (2016), New constraints on upper mantle creep mechanism inferred from silicon grain-boundary diffusion rates, *Earth Planet. Sci. Lett.*, *433*, 350–359.

Gung, Y., M. Panning, and B. Romanowicz (2003), Global anisotropy and the thickness of continents, *Nature*, *422*(6933), 707–711.

Hirth, G., and D. Kohlstedt (2003), Rheology of the upper mantle and the mantle wedge: A view from the experimentalists, in *Inside the Subduction Factory* edited by J. Eiler, pp. 83–105, AGU, Washington, D. C.

Jaoul, O., M. Poumellec, C. Froidevaux, and A. Havette (1981), Silicon diffusion in forsterite: A new constraint for understanding mantle deformation, *Anelasticity Earth*, 95–100.

Jung, H., W. Mo, and H. W. Green (2009), Upper mantle seismic anisotropy resulting from pressure-induced slip transition in olivine, *Nat. Geosci.*, *2*(1), 73–77.
Karato, S. i. (1992), On the Lehmann discontinuity, *Geophys. Res. Lett.*, *19*(22), 2255–2258, doi:10.1029/92GL02603.
Karato, S., and M. Ogawa (1982), High-pressure recovery of olivine: Implications for creep mechanisms and creep activation volume, *Phys. Earth Planet. Inter.*, *28*(2), 102–117.
Karato, S.-I. (2012), *Deformation of Earth Materials: An Introduction to the Rheology of Solid Earth*, Cambridge Univ. Press, Cambridge, U. K.
Karato, S.-I., and D. C. Rubie (1997), Toward an experimental study of deep mantle rheology: A new multianvil sample assembly for deformation studies under high pressures and temperatures, *J. Geophys. Res.*, *102*(B9), 20,111–20,122, doi:10.1029/97JB01732.
Karato, S.-I., and H. Jung (2003), Effects of pressure on high-temperature dislocation creep in olivine, *Philos. Mag.*, *83*(3), 401–414.
Karato, S.-I., D. C. Rubie, and H. Yan (1993), Dislocation recovery in olivine under deep upper mantle conditions: Implications for creep and diffusion, *J. Geophys. Res.*, *98*(B6), 9761–9768, doi:10.1029/93JB00472.
Kawazoe, T., S.-i. Karato, K. Otsuka, Z. Jing, and M. Mookherjee (2009), Shear deformation of dry polycrystalline olivine under deep upper mantle conditions using a rotational Drickamer apparatus (RDA), *Phys. Earth Planet. Inter.*, *174*, 128.
Kohlstedt, D., H. Nichols, and P. Hornack (1980), The effect of pressure on the rate of dislocation recovery in olivine, *J. Geophys. Res.*, *85*(B6), 3122–3130, doi:10.1029/JB085iB06p03122.
Mainprice, D., A. Tommasi, H. Couvy, P. Cordier, and D. J. Frost (2005), Pressure sensitivity of olivine slip systems and seismic anisotropy of Earth's upper mantle, *Nature*, *433*(7027), 731–733.
Montagner, J. P., and B. L. N. Kennett (1996), How to reconcile body-wave and normal-mode reference Earth models, *Geophys. J. Int.*, *125*(1), 229–248.
Nettles, M., and A. M. Dziewonski (2008), Radially anisotropic shear velocity structure of the upper mantle globally and beneath North America, *J. Geophys. Res.*, *113*, B02303, doi:10.1029/2006JB004819.
Ohuchi, T., T. Kawazoe, Y. Nishihara, N. Nishiyama, and T. Irifune (2011), High pressure and temperature fabric transitions in olivine and variations in upper mantle seismic anisotropy, *Earth Planet. Sci. Lett.*, *304*(1–2), 55–63.
Paterson, M. (1982), The determination of hydroxyl by infrared absorption in quartz, silicate glasses, and similar materials, *Bull. Soc. Fr. Mineral.*, *105*, 20–29.
Raterron, P., J. Chen, L. Li, D. Weidner, and P. Cordier (2007), Pressure-induced slip-system transition in forsterite: Single-crystal rheological properties at mantle pressure and temperature, *Am. Mineral.*, *92*(8-9), 1436–1445.
Raterron, P., E. Amiguet, J. Chen, L. Li, and P. Cordier (2009), Experimental deformation of olivine single crystals at mantle pressures and temperatures, *Phys. Earth Planet. Inter.*, *172*(1–2), 74–83.
Raterron, P., J. Chen, T. Geenen, and J. Girard (2011), Pressure effect on forsterite dislocation slip systems: Implications for upper-mantle LPO and low viscosity zone, *Phys. Earth Planet. Inter.*, *188*(1–2), 26–36.
Visser, K., J. Trampert, S. Lebedev, and B. L. N. Kennett (2008), Probability of radial anisotropy in the deep mantle, *Earth Planet. Sci. Lett.*, *270*(3–4), 241–250.
Wang, L., S. Blaha, Z. Pintér, R. Farla, T. Kawazoe, N. Miyajima, K. Michibayashi, and T. Katsura (2016), Temperature dependence of [100](010) and [001](010) dislocation mobility in natural olivine, *Earth Planet. Sci. Lett.*, *441*, 81–90.